Time-Resolved Spectroscopic Study of the Reaction Cl + *n*-C_5H_{12} → HCl + C_5H_{11} in Solution†

Leonid Sheps, Andrew C. Crowther, Stacey L. Carrier, and F. Fleming Crim*

Department of Chemistry, University of Wisconsin—Madison, Madison, Wisconsin 53706

Received: August 5, 2005; In Final Form: September 14, 2005

We study the hydrogen abstraction reaction from pentane by chlorine radicals using four different experimental approaches. We use two different solvents (CH_2Cl_2 and CCl_4) and two different chlorine atom sources (photodissociation of dissolved Cl_2 and two-photon photolysis of the solvent) to investigate their effects on the recombination and reactivity of the chlorine radical. All four experimental schemes involve direct probing of the transient chlorine population via a charge transfer transition with a solvent molecule. In one of the four approaches, photolysis of Cl_2 in dichloromethane, we also monitor the nascent reaction products (HCl) by transient vibrational spectroscopy. Probing both the reactants and the products provides a comprehensive view of this bimolecular reaction in solution. Between one-third and two-thirds of the chlorine radicals that initially escape the solvent cage undergo diffusive geminate recombination with their partner radical (either another chlorine atom or the solvent radical). The rest react with pentane with the bimolecular rate constants $k_{bi} = (9.5 \pm 0.7) \times 10^9\ M^{-1}\ s^{-1}$ in CH_2Cl_2 and $k_{bi} = (7.4 \pm 2) \times 10^9\ M^{-1}\ s^{-1}$ in CCl_4. The recombination yield ϕ_{rec} depends on both the chlorine atom precursor and the solvent and is larger in the more viscous carbon tetrachloride solutions. The bimolecular reaction rate k_{bi} depends only on the solvent and is consistent with a nearly diffusion-limited reaction.

I. Introduction

The fundamental importance of photodissociation and bimolecular reaction has made them the focus of extensive experimental and theoretical studies, but much of the work to date has concentrated on gas phase systems. Consequently, the dynamics involved in photodissociation and reactions of isolated systems in gases are much better understood than those in condensed phases. Direct dynamical studies in solution with even moderate state resolution are experimentally challenging for several reasons. Real-time monitoring of reactions in liquids demands good time resolution, and frequent interactions often make solution phase spectra broad and congested. For example, the lifetime of a solute molecule reacting at the diffusion-limited rate with solvent molecules is about 10 ps. In addition, vibrational transitions can have widths of hundreds of wavenumbers, making detection of individual states difficult. Perhaps most important, solvent interactions can change the energetics and dynamics of the reactive system from those in the gas phase, adding another level of complexity.

There are several direct ultrafast time-resolved studies of chemical reactions in solution. Raftery et al. have studied hydrogen abstraction reactions of Cl and CN radicals in solution in the picosecond domain.[1,2] Iwata et al. have investigated the bimolecular reactions of photoexcited aromatic molecules with carbon tetrachloride using techniques such as visible and infrared absorption spectroscopy, fluorescence, and Raman spectroscopy with time resolution ranging from nanosecond to subpicosecond.[3−7] Recently, we have performed a time-resolved study of the recombination dynamics and hydrogen abstraction reactions of chlorine radicals in solution.[8] In those experiments, we used two-photon photolysis of the dichloromethane solvent to generate chlorine atoms and probed their transient absorption with subpicosecond time resolution using a strong solvent−Cl charge transfer transition centered at 340 nm. A third of the radicals that initially escape the solvent cage diffusively recombine with their geminate partner radical, CH_2Cl, and the rest react either with the solvent or with the added solute. Using this approach, we have obtained hydrogen abstraction rates that vary from activation-limited to diffusion-limited for 16 different solutes (alkanes, alcohols, and chlorinated alkanes) and interpreted the results through a diffusion-based Smoluchowski model.[9]

The detailed study of chlorine radical dynamics in solution that we describe here extends our previous work and has two distinct goals. The first is to develop a comprehensive picture of the hydrogen abstraction reaction of Cl with pentane, Cl + *n*-pentane → C_5H_{11} + HCl, by probing both the reactants and the products under similar experimental conditions. In detecting HCl, we take advantage of the spectral window present in the IR absorption of pentane at about 2780 cm^{-1}. The second goal is to explore the effect of the solvent and the Cl precursor on subsequent chlorine dynamics in four different experimental schemes with an eye toward developing general approaches to study bimolecular reaction dynamics in solution. Because the reaction of Cl atoms with pentane is nearly diffusion-limited, we can explore the predicted influence of solvent viscosity on the reaction rate constant. We use two different solvents (CH_2Cl_2 or CCl_4) and employ two different schemes to generate chlorine radicals (two-photon photolysis of the solvent at 267 nm or photodissociation of dissolved molecular chlorine, Cl_2, at 350 nm). Table 1 summarizes the solvent, Cl source, photolysis method, and probe technique used in the four different approaches. In each case, we monitor the transient chlorine decay and observe diffusive geminate recombination and hydrogen abstraction reactions that are consistent with the

† Part of the special issue "Jürgen Troe Festschrift".

* Corresponding author. E-mail: fcrim@chem.wisc.edu.

10.1021/jp0543835 CCC: $33.50
Published on Web 11/03/2005

TABLE 1: Summary of Experimental Approaches

scheme	solvent	Cl• precursor	photolysis method	species probed	probe method
I	CH_2Cl_2	Cl_2	1-photon (350 nm)	reactants (Cl•) products (HCl)	CT[a] (330 nm) $v = 1 \leftarrow 0$ (3.6 μm)
II		solvent	2-photon (267 nm)	reactants (Cl•)	CT (330 nm)
III	CCl_4	Cl_2	1-photon (350 nm)	reactants (Cl•)	CT (330 nm)
IV		solvent	2-photon (267 nm)	reactants (Cl•)	CT (330 nm)

[a] CT is a charge transfer transition where a solvent molecule and a chlorine atom act as electron donor and acceptor, respectively.

Smoluchowski model. The rate and extent of geminate recombination depend on both the solvent and the chlorine atom precursor, but the rate of reaction with pentane depends only on the solvent environment, being smaller in the more viscous carbon tetrachloride solutions. In the case of dissociation of Cl_2 in dichloromethane (experimental scheme I in Table 1), we also monitor the HCl reaction products by transient infrared absorption spectroscopy. The growth of the HCl product matches the chlorine radical decay, consistent with hydrogen abstraction being the dominant Cl loss pathway. Monitoring the HCl population completes the picture of this bimolecular reaction and supports our diffusion-based analysis of chlorine radical dynamics in solution.

II. Experimental Approach

Our experiment requires a photolysis laser pulse to generate a transient chlorine radical population in solution and a probe pulse to monitor either the loss of Cl or appearance of HCl. We produce the chlorine atoms either by two-photon dissociation of the solvent at 267 nm or by photolysis of molecular chlorine at 350 nm and probe the disappearing chlorine radicals on a charge transfer transition, centered at about 340 nm in both dichloromethane and carbon tetrachloride, that involves the complex of Cl with the solvent.[10,11] For product detection, we tune an infrared laser pulse to 3.6 μm to monitor the fundamental vibration of HCl.

The experiments use a Ti:sapphire regenerative amplifier (Coherent Legend HE) pumped by an Nd:YLF laser (Coherent Evolution 30) and seeded by a Coherent Vitesse oscillator. The amplifier produces a 1 kHz train of laser pulses centered at 800 nm with 2.5 mJ of energy and a duration of 100 fs. For two-photon photolysis of the solvent (experimental schemes II and IV in Table 1), we frequency triple a portion of the amplified 800 nm light by doubling it in a β-barium borate (BBO) crystal (type I, 0.3 mm, $\theta = 29°$) and then mixing with residual 800 nm light in another BBO crystal (type I, 0.3 mm, $\theta = 42°$) to produce about 2 μJ pulses of 267 nm light. For photolysis of Cl_2 in experimental schemes I and III, we take the 1.26 μm signal from a double-pass BBO optical parametric amplifier (OPA) (type II, 5 mm, $\theta = 27°$), then double it and mix it with the 800 nm fundamental in two successive BBO crystals (type I, 1 mm, $\theta = 22°$ and $\theta = 29°$, respectively) to make up to 10 μJ pulses of 350 nm light. To probe the chlorine atom decay, we double the 800 nm fundamental and use the resulting 400 nm light to pump a noncollinear optical parametric amplifier (NOPA)[12] based on a type I, 1 mm, $\theta = 29°$ BBO crystal. We double the signal out of the NOPA to produce near-ultraviolet pulses that are tunable over the solvent−Cl charge transfer band. To probe the appearance of HCl (experimental scheme I), we use idler pulses in the 3.6 μm region from a $KNbO_3$ OPA (type I, 2 mm, $\theta = 41.5°$).

We focus the photolysis and probe beams to about 200 and 100 μm diameters, respectively, and overlap them at a small angle in the sample to obtain a measured time resolution of about 600 fs. Two photodiodes (reference and signal) detect the probe light before and after the sample to correct for power fluctuations. Because the spectrum of the broadband infrared pulse used to detect HCl is wider than the vibrational transition of HCl, we disperse both the signal and reference pulses in a 0.25 m monochromator with 15 cm^{-1} resolution. A computer-controlled translation stage introduces a variable delay between the photolysis and probe pulses, and a chopper blocks every other photolysis pulse for active background subtraction.

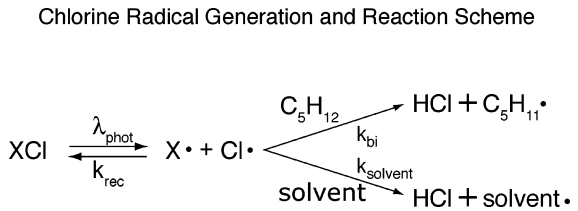

Figure 1. Chlorine radical reaction and recombination following the dissociation of a precursor XCl (X = Cl, CH_2Cl, or CCl_3). λ_{phot} is the photolysis laser wavelength, k_{rec} denotes the diffusive geminate recombination, $k_{solvent}$ is the rate constant for reaction with solvent, and k_{bi} is the rate constant for reaction with pentane.

A Teflon gear pump circulates the sample solutions through a 1 mm thick flow cell with CaF_2 windows. When used as a precursor for generating chlorine radicals, the dissolved molecular chlorine contacts a small area of stainless steel inside the gear pump. Although steel surfaces catalyze the dissociation of Cl_2 and contaminate our samples, active background subtraction removes their absorption from the transient signal. However, because accumulated decomposition products could absorb a portion of the photolysis light and interfere with chlorine atom production, we discard samples when they show signs of increased absorption at 350 nm. For photolysis of Cl_2, we bubble gaseous molecular chlorine (AGA, 99.5%) through a continuously stirred solvent and monitor its concentration in a 1 mm quartz cell using a conventional spectrometer until we achieve sufficient optical density at 350 nm. We use HPLC grade solvents (CH_2Cl_2 and CCl_4) and anhydrous pentane (99+%) without further purification.

III. Kinetic Analysis

We analyze our data with a variant of the diffusion-based Smoluchowski model.[9,13] Figure 1 shows the pathways for chlorine radical decay in our experiment, which are recombination with its geminate dissociation partner, reaction with solvent molecules, and reaction with the pentane solute. The stepwise analysis of the Cl signal is similar to the one we used previously,[8] where we first fit the transient absorption in samples with no pentane to obtain the parameters for diffusive geminate recombination and for reaction with the solvent. We then fit the traces from solutions containing pentane, holding the parameters for recombination and reaction with solvent fixed. With the chlorine decay parameters in hand, we fit the HCl rise to the same diffusion-based model.

A. Transient Cl Signal. *1. Pure Solvent.* We use the strong solvent−Cl charge transfer transition shown in the upper panel of Figure 2 to monitor the transient chlorine population in

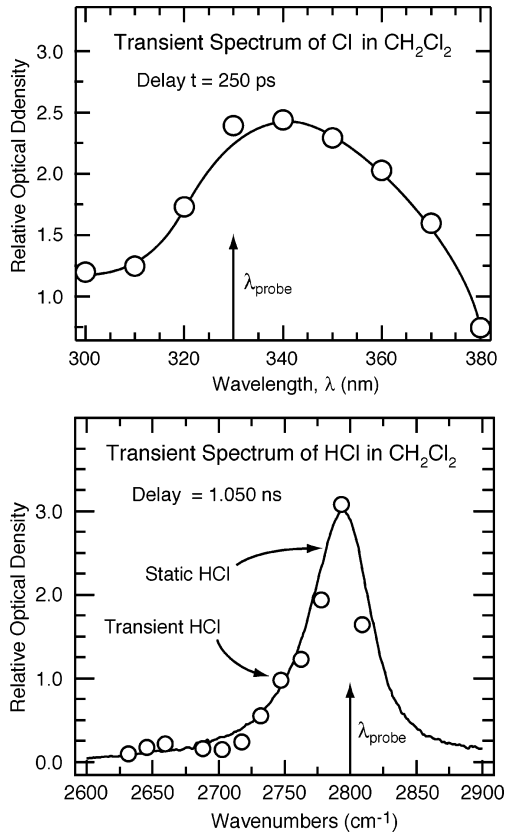

Figure 2. Upper panel: transient UV spectrum at a delay $t = 250$ ps following photodissociation of Cl_2 in CH_2Cl_2 that shows the Cl−solvent charge transfer transition. The solid line is only to guide the eye. Lower panel: transient IR spectrum 1.050 ns after photodissociation of Cl_2 in CH_2Cl_2 that shows the fundamental vibrational transition of HCl. The solid line is the equilibrium FTIR spectrum of HCl in dichloromethane.

solution.[10,11] With no pentane in the sample, solvated chlorine radicals either recombine diffusively, which leads to a fast nonexponential decay of the signal, or react with the solvent, which produces a slow exponential decay.[8] We average several traces obtained in the solvent alone and fit them to the normalized time-dependent survival probability $P_{solvent}(t)$ for chlorine radicals,[9]

$$P_{solvent}(t) = \left[1 - \phi_{rec}\,\mathrm{erfc}\left(\frac{A}{\sqrt{t}}\right)\right]\exp(-k_{solvent}t) \qquad (1)$$

where $\phi_{rec} \equiv R_{rec}/r_0$ and $A \equiv (r_0 - R_{rec})/(4D_{rec})^{1/2}$. The term in brackets arises from diffusive geminate recombination. After thermalizing at a relative distance r_0, the dissociation fragments move randomly with a relative diffusion constant D_{rec} and recombine if they approach to within an effective radius R_{rec}. We assume the simplest case of a single separation distance r_0 for all photofragment pairs although more sophisticated approaches (such as using a Gaussian distribution centered at $\langle r_0 \rangle$) are possible.[14,15] The ratio R_{rec}/r_0 is the asymptotic recombination yield ϕ_{rec},[9,13] which we obtain directly from the fits. In our experiments, ϕ_{rec} determines the extent of the chlorine radical recombination, and A determines its shape at early times. These two parameters are completely uncorrelated, which makes the fits very robust. We obtain the values of R_{rec} and r_0 from the two fitting parameters and from D_{rec}, the sum of the individual diffusion constants of the dissociation fragments. We calculate each diffusion constant using the Stokes−Einstein equation $D = k_BT/6\pi\eta\alpha$, where η is the solvent viscosity and α is the radius of the diffusing particle. Because we use the simple Stokes−Einstein equation and estimate the particle sizes from covalent radii or molar volumes, our diffusion constants are approximate, and the resulting values of r_0 and R_{rec} are only suitable for qualitative comparison. By contrast, ϕ_{rec} is a quantitatively reliable parameter.

The exponential decay in $P_{solvent}(t)$ comes from reaction with the solvent molecules and contains the corresponding rate constant. The possible Cl radical reaction pathways with the solvent are chlorine abstraction and hydrogen abstraction. We have previously measured the bimolecular rate constant for hydrogen abstraction from neat CH_2Cl_2 to be $(1.36 \pm 0.06) \times 10^7$ M^{-1} s^{-1}, which corresponds to a pseudo-first-order rate constant of 0.21 ns^{-1} and a Cl radical lifetime of 4.7 ns in dichloromethane.[8] By contrast, the Cl lifetime in neat carbon tetrachloride is about 170 ns,[16] indicating that the chlorine abstraction rate is very slow. Thus, we neglect the chlorine abstraction from either solvent and use $k_{solvent} = 0.21$ ns^{-1} for the reaction with CH_2Cl_2 and $k_{solvent} = 0$ for CCl_4.

2. Pentane Solute. Immediately after the formation of Cl radicals, the average pentane concentration around them is greater than in the steady state that characterizes the bulk reaction. The rapid reaction of this "excess" pentane with chlorine relaxes the distribution of pentane to form the steady state gradient. Consequently, Smoluchowski theory predicts a time-dependent bimolecular rate coefficient that results in nonexponential initial decay of the chlorine population.[9] The normalized survival probability of chlorine radicals reacting with pentane is

$$P_{solute}(t) = \exp\left\{-4\pi R_{rxn}D_{rxn}C_{pentane}\left(1 + \frac{2R_{rxn}}{\sqrt{\pi D_{rxn}t}}\right)t\right\} \qquad (2)$$

In this expression, R_{rxn} is the effective radius at which the reaction occurs with unit probability, D_{rxn} is the relative diffusion constant of the reactants, and $C_{pentane}$ is the concentration of the solute. The time dependence of the reaction rate coefficient $k_{bi}(t)$ is important at times less than 200 ps, but at later times, it simplifies to the steady state rate constant k_{bi},

$$k_{bi} \equiv k_{bi}(t)|_{t\to\infty} = 4\pi R_{rxn}D_{rxn}\left(1 + \frac{2R_{rxn}}{\sqrt{\pi D_{rxn}t}}\right)|_{t\to\infty} = 4\pi R_{rxn}D_{rxn} \qquad (3)$$

The time-dependent term in $k_{bi}(t)$ links the two parameters D_{rxn} and R_{rxn}, and letting them vary independently can yield a variety of unphysical values for both of them, even though their product, the bimolecular rate constant, is essentially the same. Thus, we again calculate D_{rxn} from the Stokes−Einstein equation and obtain very good and stable fits to the temporal evolution of the chlorine signal with only one adjustable parameter, R_{rxn}. As before, the approximate calculation of D_{rxn} makes the value of R_{rxn} only a qualitative estimate whose exact value depends on the calculation of the diffusion constant. By contrast, the important physical quantity that we extract from the analysis, the asymptotic bimolecular rate constant, is quantitatively robust.

Combining the expressions for the survival probability of Cl in the presence of both solvent and added solute gives the normalized time-dependent chlorine concentration,

$$\frac{[Cl](t)^{(n)}}{[Cl](0)} = P_{solvent}(t)\,P^{(n)}_{solute}(t) + S^{(n)}_{\infty} \qquad (4)$$

The parameter S_∞ is a small long-time offset with a magnitude of no more than a few percent of the initial chlorine signal and

probably comes from the absorption by a secondary radical R$^\bullet$ (R = $CHCl_2$, CH_2Cl, or C_5H_{11}) or the corresponding peroxy radical, ROO$^\bullet$, formed by reaction with dissolved oxygen.[11,17] The superscript (n) refers to the three different concentrations of pentane in our experiments (0.15, 0.3, and 0.6 M). We fit the observed Cl transient absorption signal for all pentane concentrations simultaneously using a single value of R_{rxn}.

B. Transient HCl Signal. The lower panel of Figure 2 shows a transient infrared spectrum of our sample 1.050 ns after the photolysis of Cl_2 in dichloromethane. Despite some spectral interference from the solvent and from pentane, we are able to observe the fundamental vibrational transition of HCl centered at 2780 cm^{-1} and tune our infrared probe pulse to the center of this band to monitor the HCl reaction products. As Figure 1 shows, two of the three parallel loss pathways for the chlorine radical form HCl. As usual in a parallel kinetic scheme, the rate coefficient for HCl production depends on all three pathways, and three coupled differential equations describe the HCl evolution. Numerical integration of these coupled equations shows that the dominant contribution to the HCl absorption signal comes from reaction with pentane even at its lowest concentration. Thus, to a very good approximation, the growth of the HCl signal, [HCl](t), is the complement of the reactive chlorine decay,

$$[\mathrm{HCl}](t)^{(n)} = A_{\mathrm{HCl}}^{(n)}[1 - P_{\mathrm{solute}}(t)] + S_{\infty}^{(n)} \qquad (5)$$

where $P_{solute}(t)$ is from eq 2, A_{HCl} is a scale factor, and S_∞ is a small offset. As before, (n) refers to the different concentrations of pentane in our experiments. Because we obtain all of the reaction parameters in $P_{solute}(t)$ from fitting the chlorine decay, A_{HCl} and S_∞ are the only adjustable parameters in fitting the HCl time evolution.

IV. Results and Discussion

A. Probing Reactants and Products. The first aim of this study is to obtain a full picture of the reaction of Cl with pentane in solution by monitoring both the disappearance of reactants and formation of products, which we have done by observing the chlorine radical decay and the HCl appearance following photolysis of Cl_2 in dichloromethane (experimental scheme I). The upper panel in Figure 3 shows the transient Cl signals for three different concentrations of pentane, 0.15, 0.3, and 0.6 M, and the fits to the Smoluchowski model. Immediately after the photolysis of Cl_2, we observe the charge transfer transition characteristic of solvated chlorine atoms in dichloromethane.[10,11] The chlorine radical is probably not truly free but instead is in a weakly bound ground state complex with a solvent molecule.[18] In the first 2 ps the chlorine signal rises slightly, probably reflecting the thermalization of the these solvent complexes,[19] and we limit our analysis to times $t \geq 2$ ps to focus on their recombination and reaction with pentane. The fits are very good and yield a bimolecular rate constant $k_{bi} = (9.6 \pm 0.4) \times 10^9$ M^{-1} s^{-1}, which correspond to a reaction radius $R_{rxn} = (0.45 \pm 0.02)$ nm, calculated using our estimate of the diffusion constant. The diffusive geminate recombination pathway accounts for the loss of about half of the chlorine atoms in the first 100 ps, after which it does not further influence the time evolution. Table 2 summarizes all of the fit parameters.

The very intense solvent−Cl charge transfer transition allows us to observe even low chlorine radical concentrations easily. Using a photolysis pulse energy of only 1.7 μJ and an initial Cl_2 concentration that gives an optical density of 0.37 at 350 nm, we obtain asymptotic chlorine signals of about 20 mOD in the absence of pentane. By contrast, absorption on the vibrational transition of HCl is much weaker, and its detection requires large concentrations. In the HCl detection experiments, we use 10.4 μJ pulses of the 350 nm photolysis light and a sample with an optical density of 1.2, corresponding to a 10-fold increase in the initial Cl radical concentration. Even though all of the chlorine atoms that do not recombine react with pentane, the asymptotic HCl signal is only about 1.5 mOD, which gives an absorption cross-section that is approximately 130 times smaller for HCl than for the chlorine−solvent complex. Using a gas-phase extinction coefficient $\epsilon \approx 30$ M^{-1} cm^{-1} for HCl,[2] we calculate the extinction coefficient of Cl in dichloromethane to be about 4000 M^{-1} cm^{-1}, in sensible agreement with the value of 3750 M^{-1} cm^{-1} recently reported for Cl radicals in water.[15]

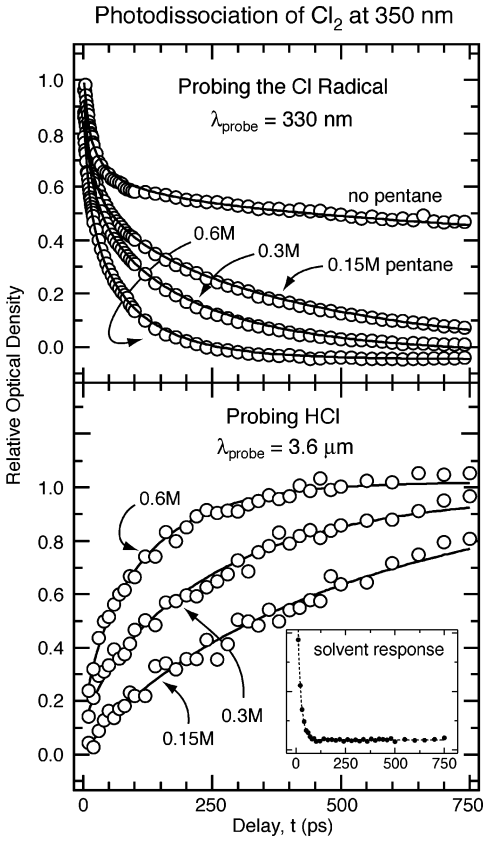

Figure 3. Transient signals from the Cl radical (upper panel) and HCl (lower panel) following photodissociation of Cl_2 in CH_2Cl_2, corresponding to experimental scheme I. The solid lines are the fits to the kinetic model.

The lower panel in Figure 3 shows the transient HCl signals for the reaction of Cl with pentane in dichloromethane. The solvent response dominates the transient signal in the 2800 cm^{-1} region at early times, as shown in the inset in Figure 3. This response, consisting of an instrument-limited rise and an exponential decay with a 17 ps lifetime, does not require the presence of pentane or Cl_2 in the solution. Because dichloromethane has a weak absorption in this region, it is possible that two-photon excitation followed by fast internal conversion and subsequent vibrational cooling produces this solvent transient. The background response is the same for all samples, and we scale it to match the early-time transient absorption and subtract it from our infrared traces. The points in the bottom panel are the resulting HCl transient signal for the same pentane concentrations as in the experiments detecting Cl (0.15, 0.3, and 0.6 M), and the solid lines are fits to the kinetic model (eq 5). The HCl population rise nearly mirrors the reactive decay

TABLE 2: Fit Parameters for Chlorine Radical Decay

		solvent:	CH_2Cl_2	CH_2Cl_2	CCl_4	CCl_4
		$Cl^•$ precursor:	Cl_2	solvent	Cl_2	solvent
		reaction scheme:	I	II	III	IV
fixed parameters	D_{rec} ($nm^2\ ns^{-1}$)		2.72	4.3	1.1	1.3
	D_{rxn} ($nm^2\ ns^{-1}$)		2.83	2.83	1.22	1.22
	$k_{solvent}$ (ns^{-1})		0.21	0.21	0	0
adjustable parameters	ϕ_{rec}		0.52 ± 0.03	0.32 ± 0.01[a]	0.65 ± 0.04	0.60 ± 0.04
	A ($ns^{-1/2}$)		0.071 ± 0.017	0.082 ± 0.005[a]	0.056 ± 0.014	0.072 ± 0.025
	R_{rxn} (nm)		0.45 ± 0.02	0.43 ± 0.03[a]	0.78 ± 0.04	0.83 ± 0.23
calculated parameters	r_0 (nm)		0.49 ± 0.15	0.50 ± 0.05[a]	0.34 ± 0.11	0.41 ± 0.17
	R_{rec} (nm)		0.25 ± 0.08	0.16 ± 0.02[a]	0.22 ± 0.07	0.25 ± 0.1
	k_{bi} ($10^9\ M^{-1}\ s^{-1}$)		9.6 ± 0.4	9.3 ± 0.7[a]	7.2 ± 0.4	7.7 ± 2.1

[a] Values taken from ref 8. All uncertainties are $\pm 1\sigma$.

of the chlorine radicals. Most important, the value of $k_{bi} = 9.6 \times 10^9\ M^{-1}\ s^{-1}$ that we determine from the chlorine decay produces an excellent fit to the HCl transients. (Letting k_{bi} vary results in values that are only slightly smaller, and still within our experimental uncertainty.) The only free parameters are the amplitudes for the three different pentane concentrations, which are the same to within about 4%, and a small offset that likely comes from solvent heating. The relative amplitudes of the transient HCl signals are consistent with our conclusion that the diffusive geminate recombination is important only for the first 100 ps and does not compete appreciably with the slower hydrogen abstraction. The consistency of the rate constants obtained by monitoring HCl products and Cl reactants demonstrates the utility of the sensitive transient absorption of the Cl−solvent complex for probing the fast reaction kinetics.

B. Influence of Solvent and Cl Precursor. The second aim of this study is to test the influence of different Cl radical precursors and different solvents, summarized in Table 1, on the decay of the Cl signal. Experimental scheme II (two-photon dissociation of dichloromethane) is identical to our previous work,[8] but we use slightly different pentane concentrations here and find that the results agree well. Experimental schemes III and IV use the same chlorine radical sources as I and II, but in carbon tetrachloride, which is a more viscous solvent (0.908 cP versus 0.413 cP).[20] Figure 4 shows the transient chlorine signal we obtain using experimental schemes II−IV along with the fits using the parameters in Table 2. Two trends are obvious in the results: the bimolecular reaction rate constants (k_{bi}) depend only on the solvent, and the geminate recombination parameters (ϕ_{rec} and A) depend on both the solvent and the precursor.

1. Reaction Rate Constants. The bimolecular rate constants and, hence, the calculated reaction radii R_{rxn} are the same within their uncertainties in the two experiments in dichloromethane, as are the two obtained in carbon tetrachloride. The dependence on only the solvent and not the Cl precursor shows that the source of the chlorine radicals does not influence the rate of the reaction of Cl with pentane. Because we use low pentane concentrations, our hydrogen abstraction reactions take hundreds of picoseconds, and the thermal chlorine radical retains no signature of its initial recoil energy or dissociation partner. The bimolecular rate constants k_{bi} of about $9.5 \times 10^9\ M^{-1}\ s^{-1}$ in dichloromethane and $7.4 \times 10^9\ M^{-1}\ s^{-1}$ in carbon tetrachloride are consistent with a nearly diffusion-limited reaction, with the latter rate constant being smaller because CCl_4 is a more viscous solvent. In the gas phase, the reaction of chlorine radicals with pentane has a large, temperature-independent rate constant $k_{gas} = (1.5 \pm 0.01) \times 10^{11}\ M^{-1}\ s^{-1}$, implying that there is little or no energy barrier[21−23] in analogy to the largely diffusion-controlled reactions we observe in both solutions.

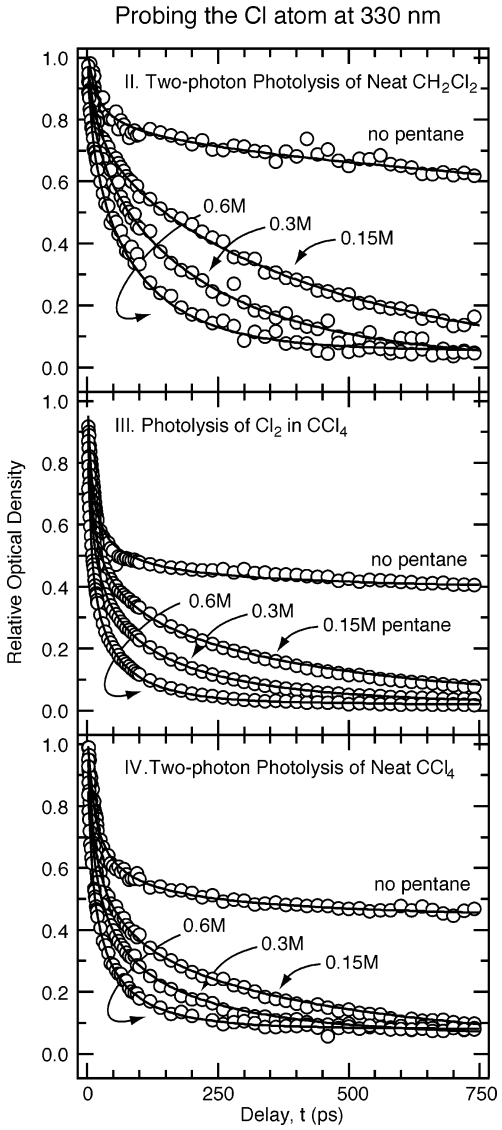

Figure 4. Transient Cl radical signals following two-photon photolysis of the solvent CH_2Cl_2, photodissociation of Cl_2 in CCl_4, and two-photon photolysis of the solvent CCl_4, corresponding to experimental schemes II−IV. The solid lines are the fits to the kinetic model.

The ratio of reaction rates in CH_2Cl_2 and CCl_4 is only 1.3, even though the ratio of the viscosities of the two solvents is about 2.2 at room temperature. The size of the reactants is similar in both cases, and therefore, their diffusion-limited reaction rates should scale with solvent viscosity through the relative diffusion constants. The solvent dependence of chlorine radical reactivity may well be responsible for this discrepancy.

Chateauneuf found that the rate constants of several hydrogen abstraction reactions depend on the solvent because of weakly bound ground state Cl−solvent complexes.[18] For the activation-controlled reaction Cl + CH_2Cl_2, the rate constant is about 10 times larger in CCl_4 than in CH_2Cl_2, indicating a significantly more reactive chlorine atom. Our results also indicate a more reactive Cl−CCl_4 complex, although the effect is much smaller in the nearly diffusion-controlled reaction of Cl with pentane. Theoretical calculations of reaction barriers for different Cl complexes would help clarify this point.

2. Recombination Parameters. The recombination kinetics of the chlorine radicals depend on the details of the four different experimental approaches, and we can make several qualitative comparisons among them. Experimental schemes I and III employ the same precursor, Cl_2, in different solvents. Table 2 shows that the recombination yield ϕ_{rec} is lower in dichloromethane, indicating that more chlorine atoms escape diffusive geminate recombination. The reason for this difference in ϕ_{rec} is that the initial photolysis fragment separation r_0 is larger in CH_2Cl_2 than in CCl_4, consistent with the latter being more viscous. The recombination radius R_{rec}, on the other hand, is similar in the two solvents because the recombining species are the weakly bound chlorine−solvent complexes, which have roughly equal sizes.

Experimental schemes II and IV use two-photon photolysis of the solvent (CH_2Cl_2 or CCl_4) and show a surprisingly small initial fragment separation r_0 of about 0.5 and 0.4 nm, respectively. We calculate an excess energy of 5.8 eV in both solvents using the gas phase C−Cl bond strength of 3.5 eV,[24] but the initial separation r_0 is about the same as in the much less energetic photolysis of Cl_2, where the excess energy is only 1 eV.[2] A recent study by Madsen et al. on the photolysis of HOCl suggests that if the solvent dissociation were direct, r_0 should be much larger,[14] leading us to suspect that, following two photon excitation, both solvents rapidly internally convert to dissociative states of comparable energy. Unlike the dissociation of Cl_2, the recombination radius R_{rec} is larger in carbon tetrachloride than in dichloromethane because of the bulkier geminate recombination partner (the solvent radical CCl_3 compared to CH_2Cl). As a result, the recombination yield ϕ_{rec} in dichloromethane is lower than in carbon tetrachloride by a factor of 2.

V. Summary

We have studied the reaction of Cl radicals with pentane in dichloromethane and carbon tetrachloride using two different radical sources and monitoring either the Cl radical decay or, in one case, the appearance of HCl. Using photolysis of Cl_2 to generate Cl atoms in dichloromethane and transient electronic absorption of the Cl−solvent complex near 330 nm to monitor their decay, we determine a rate constant of $(9.5 \pm 0.7) \times 10^9$ M^{-1} s^{-1} for the H-atom abstraction reaction of Cl with pentane in CH_2Cl_2. A similar measurement in a more viscous solvent, CCl_4, gives a smaller rate constant of $(7.4 \pm 2) \times 10^9$ M^{-1} s^{-1}. Together these fast reaction rate constants point to a nearly diffusion-limited reaction. Using transient infrared absorption to monitor the HCl product of the reaction in dichloromethane gives the same bimolecular rate constant as the measurement of the Cl radial decay, and the time evolution of the products agrees with the prediction from the loss of the reactants. The sensitive observation of the consumption of Cl using electronic spectroscopy provides the same kinetic information as the more difficult detection of the HCl product albeit without the possibility of monitoring individual vibrational state populations.

An important Cl loss pathway is the diffusive geminate recombination with their dissociation partner. To explore the effect of different radical sources on the recombination kinetics, we use two-photon photolysis of the solvent in addition to photolysis of Cl_2 as a source of Cl radicals. Approximately 30−60% of the Cl atoms that initially escape the solvent cage recombine diffusively, depending on the solvent and the precursor. The initial fragment separations and the effective recombination radii qualitatively agree with a diffusion-controlled geminate recombination that takes about 100 ps. The higher energy two-photon photolysis of the solvent does not lead to a greater initial separation of the Cl atom than the one-photon photolysis of Cl_2, suggesting that the dissociation does not occur from the initially excited state but from a lower energy state reached by internal conversion. The measured bimolecular reaction rate constants are identical using either Cl source and only depend on the identity of the solvent. The diffusion-based Smoluchowski theory describes the recombination and bimolecular reaction of chlorine radicals in solution quite well, even at times as early as 2 ps and pentane concentrations as large as 0.6 M.

Acknowledgment. We thank the National Science Foundation for support of this research, and A.C.C. thanks the National Science Foundation for a predoctoral fellowship.

References and Notes

(1) Raftery, D.; Gooding, E.; Romanovsky, A.; Hochstrasser, R. M. *J. Chem. Phys.* **1994**, *101*, 8572.
(2) Raftery, D.; Iannone, M.; Phillips, C. M.; Hochstrasser, R. M. *Chem. Phys. Lett.* **1993**, *201*, 513.
(3) Iwata, K.; Hamaguchi, H.-O. *Bull. Chem. Soc. Jpn.* **1997**, *70*, 2677.
(4) Iwata, K.; Hamaguchi, H.-O. *J. Mol. Struct.* **1997**, *413*−*414*, 101.
(5) Iwata, K.; Hamaguchi, H.-O. *Chem. Lett.* **2000**, 456.
(6) Iwata, K.; Takahashi, H. *J. Mol. Struct.* **2001**, *598*, 97.
(7) Iwata, K.; Takeuchi, S.; Tahara, T. *Chem. Physics Lett.* **2001**, *347*, 331.
(8) Sheps, L.; Crowther, A. C.; Elles, C. G.; Crim, F. F. *J. Phys. Chem. A* **2005**, *109*, 4296.
(9) Rice, S. A. *Comprehensive Chemical Kinetics, Vol. 25: Diffusion-Limited Reactions*; Elsevier: Amsterdam, 1985.
(10) Chateauneuf, J. E. *Chem. Phys. Lett.* **1989**, *164*, 577.
(11) Emmi, S. S.; Beggiato, G.; Casalboremiceli, G. *Radiat. Phys. Chem.* **1989**, *33*, 29.
(12) Wilhelm, T.; Piel, J.; Riedle, E. *Opt. Lett.* **1997**, *22*, 1494.
(13) Tachiya, M. *Radiat. Phys. Chem.* **1983**, *21*, 167.
(14) Madsen, D.; Thomsen, C. L.; Poulsen, J. A.; Jensen, S. J. K.; Thogersen, J.; Keiding, S. R.; Krissinel, E. B. *J. Phys. Chem. A* **2003**, *107*, 3606.
(15) Thomsen, C. L.; Madsen, D.; Poulsen, J. A.; Thogersen, J.; Jensen, S. J. K.; Keiding, S. R. *J. Chem. Phys.* **2001**, *115*, 9361.
(16) Chateauneuf, J. E. *J. Am. Chem. Soc.* **1990**, *112*, 442.
(17) Alfassi, Z. B.; Mosseri, S.; Neta, P. *J. Phys. Chem.* **1989**, *93*, 1380.
(18) Chateauneuf, J. E. *J. Org. Chem.* **1999**, *64*, 1054.
(19) Elles, C. G.; Cox, M. J.; Barnes, G. L.; Crim, F. F. *J. Phys. Chem. A* **2004**, *108*, 10973.
(20) Chemical Rubber Company. *CRC Handbook of Chemistry and Physics*, 84th ed.; CRC Press: Boca Raton, FL, 2003.
(21) Atkinson, R.; Aschmann, S. M. *Int. J. Chem. Kinet.* **1985**, *17*, 33.
(22) Hooshiyar, P. A.; Niki, H. *I. J. Chem. Kinet.* **1995**, *27*, 1197.
(23) Lewis, R. S.; Sander, S. P.; Wagner, S.; Watson, R. T. *J. Phys. Chem.* **1980**, *84*, 2009.
(24) Tschuikow-Roux, E.; Paddison, S. *Int. J. Chem. Kinet.* **1987**, *19*, 15.